Fiber-optic Brillouin distributed sensors: from dynamic to long-range measurements

Alayn Loayssa, Javier Urricelqui, Haritz Iribas, Juan José Mompó, and Jon Mariñelarena

Universidad Pública de Navarra, Campus Arrosadía, 31006 Pamplona (Spain). alayn.loayssa@unavarra.es

Abstract

In this chapter, we introduce the current state of the art in fiber-optic distributed sensors based on the stimulated Brillouin scattering nonlinear effect. This type of sensors provides measurements of strain and temperature along every position of a standard singlemode fiber, which can be applied to monitor the health of structures in civil, geotechnical, mechanical and aerospace engineering. We start by briefly reviewing the fundamentals of the technology, focusing in its most mature version: the Brillouin optical-time domain analysis (BOTDA) sensor. The theoretical underpinnings of these sensors are discussed as well as the practical deployment of measurement setups. Then, we focus on discussing the current research trends in BOTDA sensors, particularly in two areas: dynamic sensing and long-range measurements. Dynamic BOTDA sensors are able to measure the strain distributed along a fiber that is fixed to a structure that is experiencing movement or vibration. This requires reducing the measurement time of the distributed sensor so that hundreds of measurements can be performed each second. We review the methods that have been demonstrated to achieve this performance and show some specific examples. The other research trend that we consider is the extension of the measurement range of the sensor. This is driven by applications such as oil and gas pipeline integrity monitoring or the measurement of temperature along high-voltage power lines, in which the distance to monitor can reach hundreds of kilometers. We discuss the fundamental limitations to enlarge the range of BOTDA sensors and describe the techniques that have been deployed to overcome these limitations in order to reach measurement distances over 100 km.

1 Introduction

Brillouin distributed sensors (BDS) have been extensively researched and developed in the last three decades due to their potential to measure the distribution of temperature and strain along an optical fiber, providing thousands of measurement locations along an structure in a cost-effective manner. The applications of the technology are multiple in diverse fields. For instance, in the oil and gas industry, where BDS have been applied to measure temperature and strain along the umbilical cables used for subsea wells. They have also been extensively deployed for more than a decade to assess the integrity of oil and gas pipelines regarding the detection of leaks as well as geohazard threats such as erosion, landslide and subsidence [1]. In the electric grid, BDS have been deployed for ampacity and thermal rating of high voltage cables, particularly in undeground or subsea installation [2]. In aerospace and other industries such as wind power, they can be used to measure dynamic strain of composite structures during operation or in fatigue tests. In geotechnical engineering, BDS can be installed directly in the soil for monitoring of slopes and landslides or in levees and embankments. They can also be fitted to structures such as tunnels or piles to assess their behavior in response to the soil characteristics or to nearby construction works [3]. BDS can also be deployed to detect seepage in hydraulic structures such as dams or to measure the water content of soil for agricultural applications or to regulate the irrigation systems of parks and gardens [3].

In the following, we review the fundamentals of BDS, focusing on its most successful variety: the Brillouin optical time-domain analysis (BOTDA) sensors. In addition, we discuss recent progress in the technology, focusing, first, on methods to perform the fast measurements that are needed in applications that require dynamic characterization, and then, on techniques for long-range measurement applications.

2 Fundamentals of Brillouin distributed sensors

Brillouin scattering nonlinear effect results from the interaction in a material between optical photons and acoustic phonons [5]. In optical fibers, spontaneous Brillouin scattering takes place when a narrow-band pump light interacts with thermally excited acoustic waves. Due to the acousto-optic effect, the acoustic wave generates a periodic perturbation of the refractive index that reflects part of the energy of the pump wave by Bragg diffraction. The reflected light (Stokes wave), experiences a shift in frequency due to the

Doppler effect. This is the so-called Brillouin frequency shift (BFS), which is related to the velocity of the acoustic waves in the fiber. Spontaneous Brillouin scattering can become stimulated Brillouin scattering (SBS) if a Stokes wave whose optical frequency is down-shifted from that of the pump by the BFS is injected in the fiber. In SBS, the counterpropagation of the pump and Stokes waves generates a moving interference pattern which induces an acoustic wave due to the electrostriction effect, reflecting part of the energy of the pump wave by Bragg diffraction. The frequency of the light reflected as a consequence of this process is downshifted by the BFS, which is given by:

$$BFS = \frac{2n\nu_A}{\lambda_P} \tag{1}$$

where ν_A is the velocity of the acoustic wave, n is the refractive index, and λ_P is the wavelength of the pump wave. This shift is around 10.8 GHz at a wavelength of 1550 nm for silica fibers. As a result of this interaction, there is a transfer of energy between the pump and Stokes waves that simultaneously enhances the amplitude of the acoustic waves leading to a stimulation of the process. Therefore, as the signals propagate along the fiber, the Stokes wave is amplified while the pump wave losses energy and is attenuated. In terms of spectral response, this interaction can be described by the Brillouin gain coefficient, given by:

$$g_B(\Delta\nu) = g_B \frac{(\Delta\nu_B/2)^2}{(\Delta\nu)^2 + (\Delta\nu_B/2)^2} \tag{2}$$

with g_B the peak gain coefficient, $\Delta\nu$ the detuning from the center of the Brillouin resonance and $\Delta\nu_B$ the Brillouin linewidth, which is given by the inverse of the phonon lifetime and is usually of the order of a few tens of MHz for standard singlemode fiber. When using the Brillouin scattering effect for optical fiber sensing purposes, the dependence of Brillouin parameters on temperature and strain in the fiber is exploited. This linear dependence of the BFS with the applied strain $\delta\epsilon$ or temperature change δT is given by [6]:

$$BFS - BFS_0 = A \cdot \delta\epsilon + B \cdot \delta T \tag{3}$$

where BFS_0 is the reference BFS value, measured at room temperature and in the loose state of the fiber, i.e. laid freely in order to avoid any artificial disturbances. A and B are the strain and temperature coefficients given in MHz/$\mu\epsilon$ and MHz/°C units, respectively. Typical values for these strain and temperature coefficients are around 0.05 MHz/$\mu\epsilon$ and 1 MHz/°C for most standard fibers at 1550 nm.

Therefore, the BFS in the fiber can be found by measuring the Brillouin gain spectrum (BGS) and then translating the results to temperature or strain. In order to perform this spectral measurement, a pump wave can be injected from one end of an optical fiber and a probe wave by the other, and the gain experienced by the latter can be recorded as the wavelength separation between the two waves is scanned. Finally, the strain and temperature of the fiber can be obtained from the measured Brillouin spectrum peak gain using the coefficients obtained from a previous calibration of the deployed sensing fiber. Nevertheless, this procedure would measure the global gain spectrum of the total length of fiber, which is given by the integration of the local gain (or loss) at each position along the fiber. In order to implement a distributed sensor featuring spatially-resolved measurements, the gain spectra at individual locations in the fiber must be isolated. This can be done in the time, coherence, or frequency domains, giving rise to the three main analysis BDS types: Brillouin optical time-domain analysis (BOTDA), Brillouin optical correlation-domain analysis (BOCDA) and Brillouin optical frequency-domain analysis (BOFDA). This chapter is focused on BOTDA sensors because they are most successful BDS type in terms of performance and practical application.

The fundamentals of BOTDA sensors are highlighted in Fig. 1. A CW probe wave is counterpropagated with a pump pulse. The pulse propagates along the fiber and at each location imparts Brillouin gain to the probe. Finally, the received probe signal is detected in the time domain, so that the position dependent gain can be calculated by the classical time-of-flight method. If we consider t_0 the time when the trailing end of the pump pulse enters the fiber, then the probe signal received at $t = t_0 + 2\, z/c$ has interacted with the pulse between positions z and $z + u$, where c is the speed of light in the fiber and $u = \tau\ c/2$ is the interaction length, with τ the temporal duration of the pulse. Therefore, the spatial resolution of the measurement is given by u. For instance, in order to achieve a resolution of 1 m, a pulse duration of around 10 ns must be deployed. Notice that the two factor in the expression for u is due to the fact that the pump pulse and the CW probe are counterpropagating. From the discussion above, it is clear that the time-dependent BOTDA signal can be translated to position-dependent gain by the simple relation $z = (t - t_0)\ c/2$. Therefore, as shown in the figure, it is possible to reconstruct the position-dependent Brillouin spectra distributed along the fiber by sweeping the wavelength separation between pump and probe and measuring multiple BOTDA time domain traces. Finally, strain or temperature can be quantified from the measured BFS at each position.

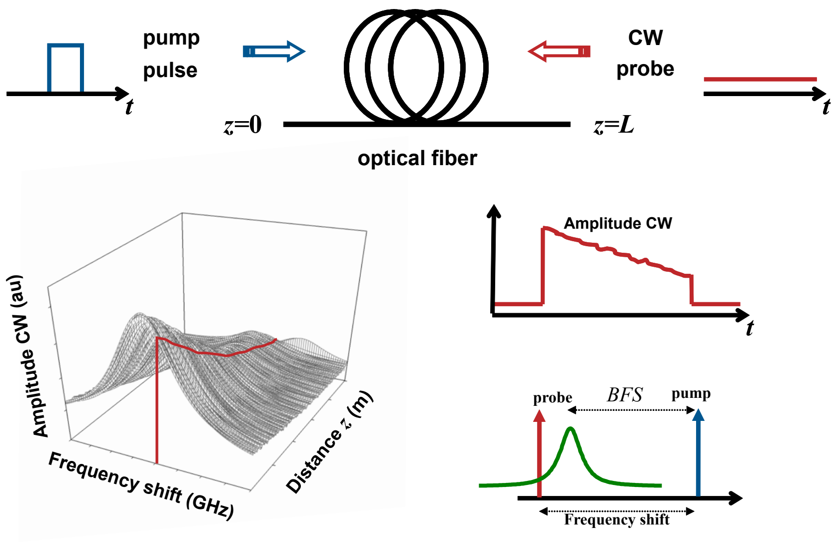

Figure 1: Fundamentals of BOTDA.

3 Research trends in BOTDA sensors

BOTDA sensor technology has reached a high degree of maturity in the last decade, coming from a time when the technology fundamentals were developed and reaching a stage in which research has been increasingly focused on enhancing the performance of the sensor system so that it can became suitable for deployment in practical applications and contribute to solve a number of industrial and societal challenges. One of the main research topics in latter years has been reducing the measurement time to provide dynamic measurements, which are needed for a number of applications in which there is a rapid variation of the measurand. Typically, this is for assessing the structural health of structures that are experiencing dynamic loads and the quantity of interest is strain. Paradigmatic examples of this applications can be found in the aerospace industry, where the performance of wings, fuselage and other elements of aircraft needs to be assessed. Another example would be wind turbines, particularly those in harsh environments such as offshore wind farms. Continuous structural monitoring of the blades and other components of those turbines can lead to significant savings in maintenance and extended operational service life.

Another area of research where a number of contributions can be found is related to developing methods to extend the distance range of the sensor. This is driven by applications in which very large structures or systems need to be measured. For instance, monitoring of pipelines, high voltage power lines or railways. These require sensing lengths that can be in the hundreds of kilometers.

3.1 Dynamic measurements

As it was explained in section 2, the measurement procedure followed in BOTDA sensors involves sweeping the frequency difference between the pump and probe waves so as to obtain the Brillouin gain spectrum along every location of the fiber. Then, the BFS is obtained after performing a regression to the experimentally measured data in order to find the frequency of the peak of these spectra. However, this is a time-consuming process that hinders the ability of BOTDA sensors to provide the dynamic measurements with the hundreds or even thousands of measurements per second that are required for applications such as fatigue testing of industrial structures or for the detection of vibrations.

In order to circumvent this limitation in the measurement time of BOTDA sensors several techniques have been proposed. For instance, the use of arbitrary waveform generation in conventional BOTDA setups to speed up the measurement process [4]. Also, the use of pump and probe waves containing multiple spectral components so that several frequencies within the Brillouin spectrum can be measured simultaneously [5][6]. However, the simplest solution to perform real-time measurements in a cost-effective manner without increasing the complexity of the BOTDA setup are probably the so-called slope-assisted methods. These are based on the frequency discriminator principle in which the probe wave optical frequency is fixed on the slope of the BGS and the amplitude of the detected signal is interrogated, so that variations of the Brillouin frequency shift (BFS) due to temperature or strain changes are translated to variations in the amplitude of the detected probe wave [7]. This measurement principle is schematically depicted in Fig. 2(a), where it can be seen that changes in the detuning of the probe wave within the BGS slope lead to changes of the detected probe power. Therefore, with this method the time-consuming frequency sweep process required by conventional BOTDA sensors is remove altogether.

However, a major issue with the slope assisted method lies in its reliance on amplitude measurements. In order to obtain correct measurements, it is necessary that the BFS to probe wave power transfer characteristic provided by the slope of the Brillouin gain spectrum remains stable. However, the amplitude of the Brillouin spectrum depends on the pump pulse power. Hence, any variation in the attenuation of the fiber under test, which is highly probable when it is affixed to an structure that is experiencing dynamic deformation, would be misinterpreted as a strain change and lead to measurement error. This is highlighted in Fig. 2(a) showing the effect of a

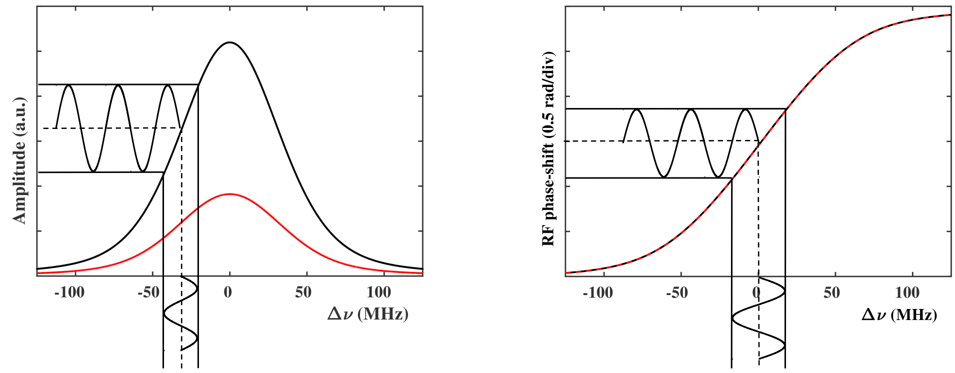

(a) (b)

Figure 2: Fundamentals of slope-assisted methods for dynamic measurements in BOTDA sensors: (a) conventional slope-assisted BOTDA based on the amplitude of the Brillouin gain spectrum, (b) BOTDA using PM and self-heterodyne detection to measured RF phase-shift.

reduction in Brillouin gain on the measurement (red line). This effect can be mitigated with a slightly modification of the the slope-assisted method in which sequential readings on both the positive and negative slopes of the BGS are performed [8]. This has been shown to increase the tolerance of the method to power variations of up to 6dB, at the cost of a doubling of the measurement time.

Nevertheless, an alternative slope-assisted BOTDA method for dynamic measurements has been proposed that greatly increases the tolerance to variations of the pump pulse power [9]. Fig. 3 depicts the fundamentals of the method, which is based on using a phase modulated probe wave and self-heterodyne detection. As it is schematically depicted in the figure, the pump wave induces a Brillouin spectrum (amplitude and phase) that is experienced by just one of the sidebands of the PM modulated probe wave. Then, the probe wave is detected in a photoreceiver generating an RF signal at the frequency of the phase modulating signal. Finally, RF demodulation is deployed to obtain the amplitude and phase-shift of that RF signal. For dynamic measurements we focus on the detected RF phase shift. Fig. 2 (b) depicts the RF phase-shift measured at a particular location in the fiber as a function of the detuning of the sideband of the PM wave from the center of the Brillouin gain spectrum. Dynamic measurements are performed by setting the pump and probe frequency difference to the center of the spectra ($\Delta\nu = 0$) so that, then, any change in BFS due to strain in the fiber is translated to

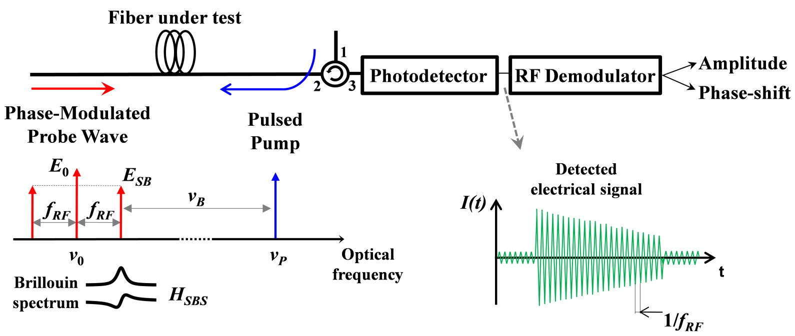

Figure 3: Fundamentals of BOTDA RF. (From Javier Urricelqui, Ander Zornoza, Mikel Sagues, and Alayn Loayssa, "Dynamic BOTDA measurements based on Brillouin phase-shift and RF demodulation," Opt. Express 20, 26942-26949 (2012). Copyright 2012 Optical Society of America).

a change in the measured RF phase-shift. A remarkable feature of this RF phase-shift spectrum is that its shape does not depend on the peak Brillouin gain or the pump pulse power [9]. This is due to the special characteristics of the detection process which involves an interference between two RF signals originaled in the beating between the optical carrier of the PM wave and each sideband. Moreover, the phase-shift in addiction to the amplitude of the Brillouin interaction spectrum intervene, in contrast to conventional BOTDA sensors that just take advantage of the amplitude response.

Fig. 4 depicts a sample dynamic measurement performed with the self-heterodyne BOTDA. A 1-m section at the end of a 930 m fiber length was fixed to a 1-m cantilever beam that was made to vibrate. In the measurement, it can be seen that only the fiber section in the cantilever beam experiences dynamic strain, while the rest of the fiber remains static. This measurement was performed with a setup that implemented a slight modification of the principle in Fig. 3 in which two pump pulses with ortogonal polarizations are deployed to simultaneously induce a gain spectrum and a loss spectrum on the upper and lower frequency sidebands, respectively, of the PM probe wave [10]. This setup provided a polarization diversity measurement of the Brillouin interaction independent of polarization induced fading. This leads to a halving of the measurement time and makes unnecessary the use of the polarization switch or scrambler that is usually deployed in BOTDA sensors.

Another limitation of slope-assisted BOTDA setups is the dynamic measurement range, i.e. the range of BFS values that can be measured with an specified precision. In the conventional slope-assisted BOTDA this is roughly given by the Brillouin spectrum linewidth. Considering a typical value for standard singlemode fiber of $\Delta\nu_B \approx 30$MHz and a strain coefficient

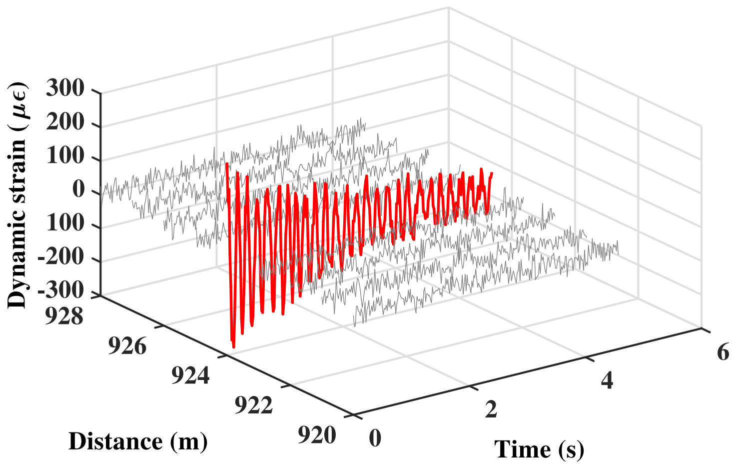

Figure 4: Dynamic measurement example. (From J. Urricelqui, F. López-Fernandino, M. Sagues and A. Loayssa, "Polarization Diversity Scheme for BOTDA Sensors Based on a Double Orthogonal Pump Interaction," in Journal of Lightwave Technology, vol. 33, no. 12, pp. 2633-2638, June 15, 2015. Copyright 2015 IEEE)

of $20\mu\epsilon$/MHz, this translates to a strain measurement range of $600\mu\epsilon$. This is insufficient for many applications in which dynamic strain of industrial parts or structures is measured. For instance, the maximum strain experienced by the blade of wind-turbine in operation is of the order of $10.000\mu\epsilon$. Moreover, the actual measurement range required in strain measurements can be even larger because the use of different fiber types or due the installation process of the fiber in the structure that can lead to the existence of a variation of BFS along the fiber even before dynamic loads are experienced.

Therefore, it is necessary to extend the measurement range for practical applications of the slope-assisted BOTDA in dynamic scenarios related to structural health monitoring. One option is switching the probe wave frequency in several steps within a given range, so that multiple BGS slopes can be interrogated [11] [12]. However, the measurement time also increases proportionally to the number of frequency steps. Another option is to deploy short pump pulses with the aim of broadening the BGS shape, which has been applied in conventional [13] as well as RF-based slope-assisted BOTDAs [14]. Fig. 5 depicts the measurement of the RF amplitude and RF phase-shift spectra in the self-heterodyne BOTDA as the pump pulse duration is reduced.

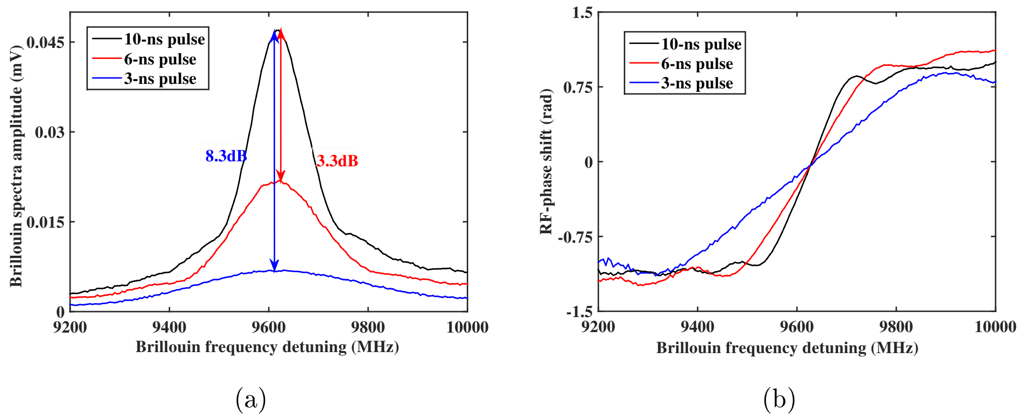

Figure 5: Experimental amplitude (a) and RF phase-shift (b) spectra when short pulses are employed. (From J. Mariñelarena, J. Urricelqui and A. Loayssa, "Enhancement of the Dynamic Range in Slope-Assisted Coherent Brillouin Optical Time-Domain Analysis Sensors," in IEEE Photonics Journal, vol. 9, no. 3, pp. 1-10, June 2017. Copyright 2017 IEEE)

Notice that the measurement range for dynamic measurements using the RF phase-shift is enhanced for shorter pulses. However, as it is shown in Fig. 5 (a) the price to pay for the increased dynamic range comes in the form of a reduction of the magnitude of the gain spectra, which leads to an equal reduction of the signal-to-noise ratio (SNR) of the measurement. In addition, it is also possible to extent the dynamic range of the RF-based slope-assisted BOTDA by launching pump pulses containing multiple frequency components [14]. This makes the Brillouin spectra generated by each component to overlap, providing a wider linear region of the detected RF phase-shift spectrum and allowing measurement of larger Brillouin frequency shift variations. Notice that this method is exclusive of the self-heterodyne BOTDA and not applicable to conventional BOTDA.

Finally, another issue that needs to be tackled with slope-assisted BOTDA sensors for dynamic operation is due to a recently found dependence of the Brillouin spectrum linewidth on the pump power [15]. This unexpected finding means that BFS measurement errors can appear in techniques such as the slope-assisted BOTDA that rely on the shape of the BGS [9]. However, it has been found that in the self-heterodyne BOTDA this effect is reduced and only becomes significant at extremely high pump powers [16].

3.2 Long-range measurements

The distance range of measurements performed using a BOTDA sensor is given by the length of sensing fiber that the system is able to measure with a specified performance in terms of measurement precision and time. This performance ultimately depends on the SNR of the probe signal received from far away locations, which in turn depends on the power of the probe and pulse pump waves that is possible to inject into the sensing fiber.

The maximum power of the pump pulse that can be injected into the sensing fiber is constrained by the onset of nonlinear effects, mainly modulation instability and Raman scattering [17]. As for the probe wave power, its maximum power in the fiber is limited firstly by the onset of so-called nonlocal effects and ultimately by the Brillouin threshold of the fiber link.

Nonlocal effects are intrinsically linked to the nature of the Brillouin interaction in a BOTDA sensor. The pump pulse gives energy to the probe wave as they counter-propagate in the sensing fiber leading to an amplification of the former that is used for sensing. However, the pump pulse is also depleted in its journey due to the energy that it loses in the interaction at each location. Moreover, this depletion depends on the BFS at every position that the pump pulse has interacted with the probe wavefronts prior to its arrival at a given location. This distorts the measured spectrum and introduces a bias in the obtained BFS that entails a systematic error in the measurement performed [18]. Notice that this measurement impairment is a nonlocal effect in the sense that the BFS measurement at a particular location in the fiber is affected by the Brillouin interaction between pump and probe at other locations.

Several methods have been proposed to mitigate nonlocal effects. An early proposal was the use of a post-processing technique for BFS reconstruction using a multidimensional minimization algorithm to determine the coefficients of a parametrized unknown profile [19]. However, this is a time-consuming process and its applicability to real-world measurements scenarios seems rather difficult. Another proposal for nonlocal effects mitigation was a time-multiplexing method that is based on pulsing the probe wave so as to limit the interaction length with the pump pulse [20][21]. However, this entails a measurement time penalty.

Altogether, the simplest and most successful alternative to mitigate nonlocal effects due to pump depletion is the use of a dual-probe setup in which two probe waves with identical separation in optical frequency from the pump are deployed [22]. These two waves induce two simultaneous Brillouin interactions (gain and loss) upon the pulse that compensate each other; hence, suppressing pulse depletion. However, this technique mitigates nonlocal effects just to first order, but there is a second-order nonlocal effect related to the appearance of linear distortion of the pump pulse spectrum due to its interaction with the two probe waves [23]. This is due to the fact that the gain and loss spectra induced by the two probe waves on the pump only overlap when their optical frequency separation equals the BFS of the fiber. However, during the spectral scan required to characterized the full BGS, the frequency separation between both waves is swept, so that for certain frequency differences the gain and loss spectra fall at different frequencies and distort the pulse spectrum, leading to measurement error.

One method to overcome second-order nonlocal effects is the use of an alternative scanning method in the dual-probe BOTDA sensor configuration in which the frequency difference between pump and probe waves is maintained so as to ensure that the gain and loss spectra induced upon the pulse continuously overlaps [24] [25]. We have also introduced a method to compensate second-order nonlocal effects that also enables dual-probe BOTDA setups to overcome the Brillouin threshold of the fiber [26]. The basis of this technique is to introduce a modulation or "dithering" to the optical frequency of the probe waves, as it is schematically depicted in Fig. 6. This makes the pump pulse to experience interaction with probe wavefronts that have a different frequency detuning, the net effect being that the integrated gain and loss spectrum generated by both probe wave broadens so that no distortion is introduced in the pump pulse spectrum and second-order nonlocal effects are suppressed [26]. A side benefit of this probe dithering method is that the optical frequency modulation of the probe waves allows to overcome the Brillouin threshold limit of the fiber. Altogether, deployment of the probe dithering method has demonstrated the largest probe wave power ever injected in a long-range BOTDA sensing link, hence enhancing the SNR of the measurements.

The probe dithering method can be used with little modification to amplify the pump pulses as they travel along the fiber; hence, increasing the sensor range. Fig. 6 hints the way to achieve this amplification. Notice that the pump pulse can be made to experience gain simply by removing the the lower optical frequency probe component. Then the higher frequency probe wave induces a broad and flat gain spectrum that equally amplifies all frequency components of the pump pulse. This technique has been demonstrated in a 100-km BOTDA sensor incorporating distributed Brillouin gain provided by the probe [27]. Fig. 7(a) depicts the BGS distribution measured along the fiber when a dual-probe BOTDA configuration with dithering is deployed. Notice that for far away locations the BGS becomes very small. Fig. 7(b) highlights the measurement of the same link, but once the lower optical frequency is removed. In this case the amplitude starts to increase

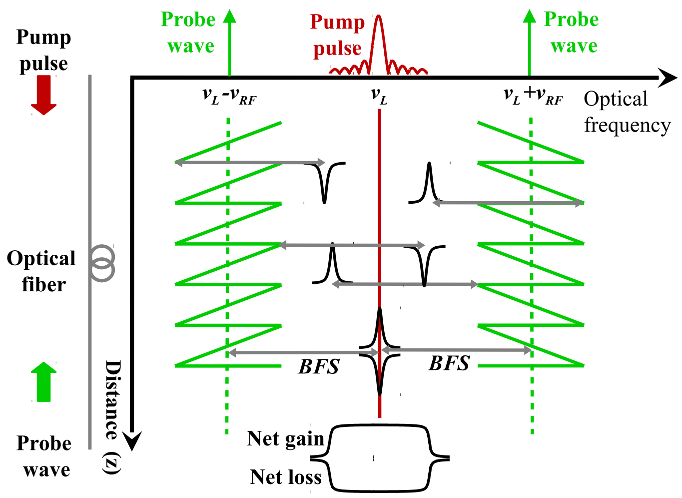

Figure 6: Fundamentals of the probe dithering technique for mitigation of second-order nonlocal effects (From R. Ruiz-Lombera, J. Urricelqui, M. Sagues, J. Mirapeix, J. M. López-Higuera and A. Loayssa, "Overcoming Nonlocal Effects and Brillouin Threshold Limitations in Brillouin Optical Time-Domain Sensors," in IEEE Photonics Journal, vol. 7, no. 6, pp. 1-9, Dec. 2015. Copyright 2015 IEEE).

and recover at mid-link when the gain provided by the probe wave starts to become significant. This amplification pump pulse can also be obtained by deploying a separated Brillouin pump source with dithering to generate distributed Brillouin gain [28].

Another method to extend to measurement range in BOTDA sensor is the use of pulse compression coding. The idea behind pulse coding is to launch into the sensing fiber coded sequences of pulses so that after detection and processing an improvement of the SNR of the retrieved single-pulse response is obtained. The first proposal for BOTDA sensors deployed the unipolar simplex coding imported from optical time-domain reflectometers [29]. This concept was latter improved deploying cyclic unipolar simplex codes that significantly reduced the measurement time because successive codewords are obtained by time-delaying a cyclic sequence [30]. The SNR enhancement brought by unipolar simplex codes is equal to $(L+1)/(2\sqrt{L})$, where L is the code length. Further refinements of pulse coding have been proposed such as using bipolar codes making simultaneous use of the gain and loss spectra [31], or deployment of so-called color coding [32], in which, the optical frequency of each pulse in the sequence is changed.

An important issue to take into account when deploying coding in BOTDA is that the successive pulses of a sequence experience an increased depletion

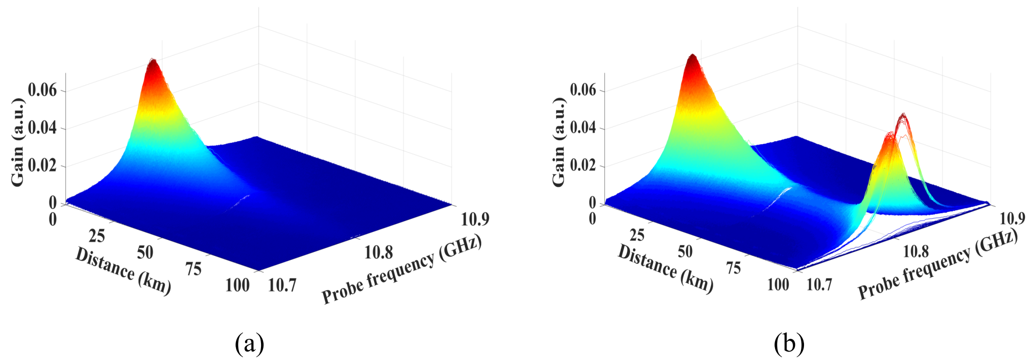

Figure 7: Brillouin gain distribution measured with (**a**) dual-probe-sideband BOTDA sensor using frequency modulation of the probe wave and (**b**) novel BOTDA with pulse amplification. A pulse duration of 45 ns was deployed in both measurements. (From Juan José Mompó, Javier Urricelqui, and Alayn Loayssa,"Brillouin optical time-domain analysis sensor with pump pulse amplification," *Opt. Express* **2016**, *24*, 12672–12681. Copyright 2016 Optical Society of America).

factor, since the n-th pulse in the sequence meets a probe wavefront that has previously been amplified by $n-1$ pulses [33]. Hence, significant levels of pump depletion will appear at lower powers in pulse-coded BOTDA setups than in conventional single-pulse BOTDA sensors. Furthermore, pulse-coded BOTDA sensors are less tolerant to a given level of pump depletion because proper decoding requires that all pulses in a sequence have identical energy. Altogether, this translates to a constrain on the length of the pulse sequences that can be deployed and hence on the maximum SNR enhancement provided by these methods. A way to mitigate this problem is to deploy a probe dithering. This has been demonstrated in a 164-km fiber loop link in which a dual-probe BOTDA setup with probe dithering deploying a 79-bit cyclic unipolar coding sequence provided 3-MHz BFS mesurement precision at 1-m spatial resolution. Fig. 8 compares a single-pulse to coded-pulse distributed probe gain measurement, where the 6.5-dB SNR enhancement associated to the code length is crearly noticeable.

4 Conclusions

In this chapter, we have reviewed the fundamentals and the latest research directions in BDSs. This technology is bound to experience increased adoption in practical application due to its unique features, particularly, after latest

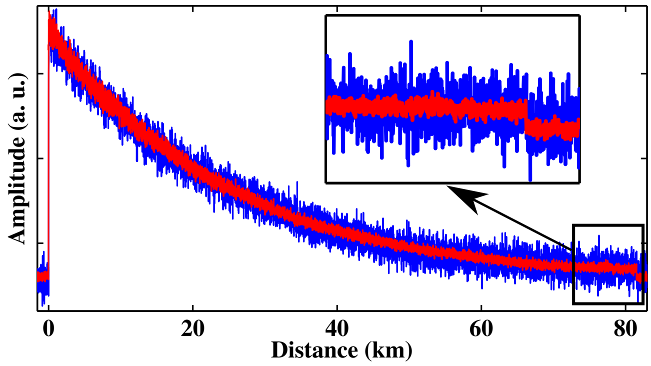

Figure 8: BOTDA traces at BFS obtained for the analyzer with a 79-bit cyclic coding (red) and without aplying coding (blue) (From Haritz Iribas, Alayn Loayssa, Florian Sauser, Miguel Llera, and Sébastien Le Floch, "Cyclic coding for Brillouin optical time-domain analyzers using probe dithering," Opt. Express 25, 8787-8800 (2017). Copyright 2017 Optical Society of America).

research efforts have greatly enhanced its performance. Future developments need to focus on developing novel application fields and in standardizing the methods for deployment of the sensors and interpretation of the measurement results.

References

[1] S. S. C. Madabhushi, M. Z. E. B. Elshafie, and S. K. Haigh, "Accuracy of distributed optical fiber temperature sensing for use in leak detection of subsea pipelines," *Journal of Pipeline Systems Engineering and Practice*, vol. 6, no. 2, p. 04014014, 2015.

[2] A. Ukil, H. Braendle, and P. Krippner, "Distributed temperature sensing: Review of technology and applications," *IEEE Sensors Journal*, vol. 12, pp. 885–892, May 2012.

[3] L. Schenato, "A review of distributed fibre optic sensors for geo-hydrological applications," *Applied Sciences*, vol. 7, no. 9, 2017.

[4] I. Sovran, A. Motil, O. Danon, and M. Tur, "An ultimately fast frequency-scanning brillouin optical time domain analyzer," in *Optical Fiber Communication Conference*, p. W2A.44, Optical Society of America, 2015.

[5] A. Voskoboinik, D. Rogawski, H. Huang, Y. Peled, A. E. Willner, and M. Tur, “Frequency-domain analysis of dynamically applied strain using sweep-free brillouin time-domain analyzer and sloped-assisted fbg sensing,” *Opt. Express*, vol. 20, pp. B581–F586, Dec 2012.

[6] C. Jin, N. Guo, Y. Feng, L. Wang, H. Liang, J. Li, Z. Li, C. Yu, and C. Lu, “Scanning-free botda based on ultra-fine digital optical frequency comb,” *Opt. Express*, vol. 23, pp. 5277–5284, Feb 2015.

[7] R. Bernini, A. Minardo, and L. Zeni, “Dynamic strain measurement in optical fibers by stimulated brillouin scattering,” *Opt. Lett.*, vol. 34, pp. 2613–2615, Sep 2009.

[8] A. Motil, O. Danon, Y. Peled, and M. Tur, “Pump-power-independent double slope-assisted distributed and fast brillouin fiber-optic sensor,” *IEEE Photonics Technology Letters*, vol. 26, pp. 797–800, April 2014.

[9] J. Urricelqui, A. Zornoza, M. Sagues, and A. Loayssa, “Dynamic botda measurements based on brillouin phase-shift and rf demodulation,” *Opt. Express*, vol. 20, pp. 26942–26949, Nov 2012.

[10] J. Urricelqui, F. López-Fernandino, M. Sagues, and A. Loayssa, “Polarization diversity scheme for botda sensors based on a double orthogonal pump interaction,” *Journal of Lightwave Technology*, vol. 33, pp. 2633–2638, June 2015.

[11] D. Ba, B. Wang, D. Zhou, M. Yin, Y. Dong, H. Li, Z. Lu, and Z. Fan, “Distributed measurement of dynamic strain based on multi-slope assisted fast botda,” *Opt. Express*, vol. 24, pp. 9781–9793, May 2016.

[12] D. Zhou, Y. Dong, B. Wang, T. Jiang, D. Ba, P. Xu, H. Zhang, Z. Lu, and H. Li, “Slope-assisted botda based on vector sbs and frequency-agile technique for wide-strain-range dynamic measurements,” *Opt. Express*, vol. 25, pp. 1889–1902, Feb 2017.

[13] Q. Cui, S. Pamukcu, W. Xiao, and M. Pervizpour, “Truly distributed fiber vibration sensor using pulse base botda with wide dynamic range,” *IEEE Photonics Technology Letters*, vol. 23, pp. 1887–1889, Dec 2011.

[14] J. Mariñelarena, J. Urricelqui, and A. Loayssa, “Enhancement of the dynamic range in slope-assisted coherent brillouin optical time-domain analysis sensors,” *IEEE Photonics Journal*, vol. 9, pp. 1–10, June 2017.

[15] A. Motil, R. Hadar, I. Sovran, and M. Tur, "Gain dependence of the linewidth of brillouin amplification in optical fibers," *Opt. Express*, vol. 22, pp. 27535–27541, Nov 2014.

[16] J. Mariñelarena, J. Urricelqui, and A. Loayssa, "Gain dependence of the phase-shift spectra measured in coherent brillouin optical time-domain analysis sensors," *Journal of Lightwave Technology*, vol. 34, pp. 3972–3980, Sept 2016.

[17] L. T. Stella M. Foaleng, "Impact of raman scattering and modulation instability on the performances of brillouin sensors," *Proc.SPIE*, vol. 7753, p. 77539V, 2011.

[18] L. Thévenaz, S. F. Mafang, and J. Lin, "Effect of pulse depletion in a brillouin optical time-domain analysis system," *Opt. Express*, vol. 21, pp. 14017–14035, Jun 2013.

[19] A. Minardo, R. Bernini, L. Zeni, L. Thevenaz, and F. Briffod, "A reconstruction technique for long-range stimulated brillouin scattering distributed fibre-optic sensors: experimental results," *Measurement Science and Technology*, vol. 16, no. 4, p. 900, 2005.

[20] Y. Dong, L. Chen, and X. Bao, "Time-division multiplexing-based botda over 100km sensing length," *Opt. Lett.*, vol. 36, pp. 277–279, Jan 2011.

[21] A. Zornoza, A. Minardo, R. Bernini, A. Loayssa, and L. Zeni, "Pulsing the probe wave to reduce nonlocal effects in brillouin optical time-domain analysis (botda) sensors," *IEEE Sensors Journal*, vol. 11, pp. 1067–1068, April 2011.

[22] A. Minardo, R. Bernini, and L. Zeni, "A simple technique for reducing pump depletion in long-range distributed brillouin fiber sensors," *IEEE Sensors Journal*, vol. 9, pp. 633–634, June 2009.

[23] A. Dominguez-Lopez, X. Angulo-Vinuesa, A. Lopez-Gil, S. Martin-Lopez, and M. Gonzalez-Herraez, "Non-local effects in dual-probe-sideband brillouin optical time domain analysis," *Opt. Express*, vol. 23, pp. 10341–10352, Apr 2015.

[24] A. Dominguez-Lopez, Z. Yang, M. A. Soto, X. Angulo-Vinuesa, S. Martin-Lopez, L. Thevenaz, and M. Gonzalez-Herraez, "Novel scanning method for distortion-free botda measurements," *Opt. Express*, vol. 24, pp. 10188–10204, May 2016.

[25] X. Hong, W. Lin, Z. Yang, S. Wang, and J. Wu, "Brillouin optical time-domain analyzer based on orthogonally-polarized four-tone probe wave," *Opt. Express*, vol. 24, pp. 21046–21058, Sep 2016.

[26] R. Ruiz-Lombera, J. Urricelqui, M. Sagues, J. Mirapeix, J. M. López-Higuera, and A. Loayssa, "Overcoming nonlocal effects and brillouin threshold limitations in brillouin optical time-domain sensors," *IEEE Photonics Journal*, vol. 7, pp. 1–9, Dec 2015.

[27] J. J. Mompó, J. Urricelqui, and A. Loayssa, "Brillouin optical time-domain analysis sensor with pump pulse amplification," *Opt. Express*, vol. 24, pp. 12672–12681, Jun 2016.

[28] J. Urricelqui, M. Sagues, and A. Loayssa, "Brillouin optical time-domain analysis sensor assisted by brillouin distributed amplification of pump pulses," *Opt. Express*, vol. 23, pp. 30448–30458, Nov 2015.

[29] M. A. Soto, G. Bolognini, F. D. Pasquale, and L. Thévenaz, "Simplex-coded botda fiber sensor with 1 m spatial resolution over a 50 km range," *Opt. Lett.*, vol. 35, pp. 259–261, Jan 2010.

[30] M. Taki, Y. Muanenda, C. J. Oton, T. Nannipieri, A. Signorini, and F. D. Pasquale, "Cyclic pulse coding for fast botda fiber sensors," *Opt. Lett.*, vol. 38, pp. 2877–2880, Aug 2013.

[31] M. A. Soto, S. L. Floch, and L. Thévenaz, "Bipolar optical pulse coding for performance enhancement in botda sensors," *Opt. Express*, vol. 21, pp. 16390–16397, Jul 2013.

[32] S. L. Floch, F. Sauser, M. Llera, M. A. Soto, and L. Thévenaz, "Colour simplex coding for brillouin distributed sensors," *Proc.SPIE*, vol. 8794, 2013.

[33] H. Iribas, A. Loayssa, F. Sauser, M. Llera, and S. L. Floch, "Cyclic coding for brillouin optical time-domain analyzers using probe dithering," *Opt. Express*, vol. 25, pp. 8787–8800, Apr 2017.